Reactivity boundaries to separate the fate of a chemical reaction associated with an index-two saddle

Yutaka Nagahata,[1,*] Hiroshi Teramoto,[1,2,†] Chun-Biu Li,[2,‡] Shinnosuke Kawai,[1,2,§] and Tamiki Komatsuzaki[1,2,‖]

[1]*Graduate School of Life Science, Hokkaido University, Kita 10 Nishi 8, Kita-ku, Sapporo 060-0810, Japan*

[2]*Molecule and Life Nonlinear Sciences Laboratory, Research Institute for Electronic Science, Hokkaido University, Kita 20 Nishi 10, Kita-ku, Sapporo 001-0020, Japan*

(Received 15 August 2012; revised manuscript received 27 May 2013; published 25 June 2013)

Reactivity boundaries that divide the destination and the origin of trajectories are of crucial importance to reveal the mechanism of reactions. We investigate whether such reactivity boundaries can be extracted for higher index saddles in terms of a nonlinear canonical transformation successful for index-one saddles by using a model system with an index-two saddle. It is found that the true reactivity boundaries do not coincide with those extracted by the transformation taking into account a nonlinearity in the region of the saddle even for small perturbations, and the discrepancy is more pronounced for the less repulsive direction of the index-two saddle system. The present result indicates an importance of the global properties of the phase space to identify the reactivity boundaries, relevant to the question of what reactant and product are in phase space, for saddles with index more than one.

DOI: 10.1103/PhysRevE.87.062817 PACS number(s): 82.20.Db, 34.10.+x, 05.45.−a, 45.20.Jj

Saddle points and the dynamics in their vicinities play crucial roles in chemical reactions. A saddle point on a multidimensional potential energy surface is defined as a stationary point at which the Hessian matrix does not have zero eigenvalues and, at least, one of the eigenvalues is negative. Saddle points are classified by the number of the negative eigenvalues, and a saddle that has n negative eigenvalues is called an *index-n saddle*. An index-one saddle on a potential surface has especially long been considered to make a bottleneck for reactions [1–3], the sole unstable direction corresponding to the "reaction coordinate." This is because index-one saddles are considered to be the lowest energy stationary point connecting two potential minima, of which one corresponds to the reactant and the other to the product, and the system must traverse the index-one saddle from the reactant to the product [4–7].

To estimate reaction rate constants across the saddles, transition state theory was proposed [1–3], by envisaging the existence of a nonrecrossing dividing surface [i.e., transition state (TS)] in the region of an index-one saddle. Recent studies of nonlinear dynamics in the vicinity of index-one saddles have revealed the firm theoretical ground for the robust existence of the no-return TS in the phase space [7–24] (see also Refs. [25,26], and references therein). The scope of the dynamical reaction theory based on normal form (NF) theory [27], a classical analog of Van Vleck perturbation theory, is not limited to only chemical reactions, but also includes, for example, ionization of a hydrogen atom under electromagnetic fields [10,11], isomerization of clusters [8,9], orbit designs in solar systems [21–24], and so forth. Very recently, these approaches have been generalized to dissipative multidimensional Langevin equations [7,14,15], laser-controlled chemical reactions with quantum effects [16,17], and systems with rovibrational couplings [18,19] and showed the robust existence of reaction boundaries even while a no-return TS ceases to exist [13].

For complex molecular systems, the potential energy surface becomes more complicated, and transitions from a potential basin to another involve not only index-one saddles but also higher index saddles [28–30]. For example, it was shown in a computer simulation of an inert gas cluster containing seven atoms that transitions from a solid-like phase to a liquid-like phase occur mostly through index-two saddles rather than through index-one saddle with the increase of kinetic temperature [29]. This indicates that the more rugged a system's energy landscape becomes and/or the more "temperature" increases, the more frequently the system contains higher index saddles.

To reveal the fundamental mechanism of the passage through a saddle with index greater than one, the phase space structure was recently studied on the basis of NF theory [31–34]. For example, the extension of the dynamical reaction theory into higher index saddles was discussed [31–33] for a stronger repulsive degree of freedom (DoF) [31,32], and a dividing surface to separate the reactant and the product was proposed for higher index saddles [34]. While these studies are of importance, the stronger repulsive DoF does not necessarily serve as the reactive direction, as shown for an index-two saddle in structural isomerization of aminoborane [28]. In addition, these studies rely on the assumption that NF performed in the region of the saddle can find the reactivity boundaries if the perturbation calculation converges [31–34].

In studies of chemical reactions, one needs to assign regions of the phase space as "reactants" or "products." Invariant manifolds in the phase space that separate the origin and the destination of trajectories have provided us with significant implications for the rate calculation and the orbit design in non-RRKM systems [7–24] (see also Refs. [25,26], and references therein). In this Letter we investigate how one can identify the reactivity boundaries to determine the fate of the reaction for higher index saddles. We analyze a two-DoF Hamiltonian system with an index-two saddle by using NF theory and investigate its applicability in determining if the

*yutaka_nagahata@mail.sci.hokudai.ac.jp
†teramoto@es.hokudai.ac.jp
‡cbli@es.hokudai.ac.jp
§skawai@es.hokudai.ac.jp
‖tamiki@es.hokudai.ac.jp

system undergoes reactions or not. We will emphasize the subtlety in defining the "reactant" and "product" regions in the phase space, and point out the difference between the regions defined by NF and those defined by the original coordinates.

If the total energy of the system is just slightly above a stationary point, the n-DoF Hamiltonian H can well be approximated by normal mode Hamiltonian H_0:

$$H(\boldsymbol{p},\boldsymbol{q}) \approx H_0(\boldsymbol{p},\boldsymbol{q}) = \sum_{j=1}^{n} \frac{1}{2}\left(p_j^2 + k_j q_j^2\right) \tag{1}$$

with normal mode coordinate $\boldsymbol{q} = (q_1,\ldots,q_n)$ and its conjugate momenta $\boldsymbol{p} = (p_1,\ldots,p_n)$, where $k_j \in \mathbb{R}$ is a "spring constant" or the curvature of the potential energy surface along the jth direction. The constants k_j can be positive or negative. If negative, the potential energy is maximum at $\boldsymbol{q} = 0$ along the jth direction. Then the direction exhibits an unstable motion corresponding to "sliding down the barrier" and can be regarded as "reaction coordinate." The index of the saddle corresponds to the number of negative k_j. Flow of the DoF with negative k_j is depicted in Fig. 1(a). Here one can introduce the following coordinates:

$$\eta_j = (p_j + \lambda_j q_j)/(\lambda_j\sqrt{2}), \quad \xi_j = (p_j - \lambda_j q_j)/\sqrt{2}, \tag{2}$$

where $\lambda_j = \sqrt{-k_j}$. When Eq. (1) holds, the action variable defined by $I_j = \xi_j\eta_j$ is an integral of motion, and trajectories

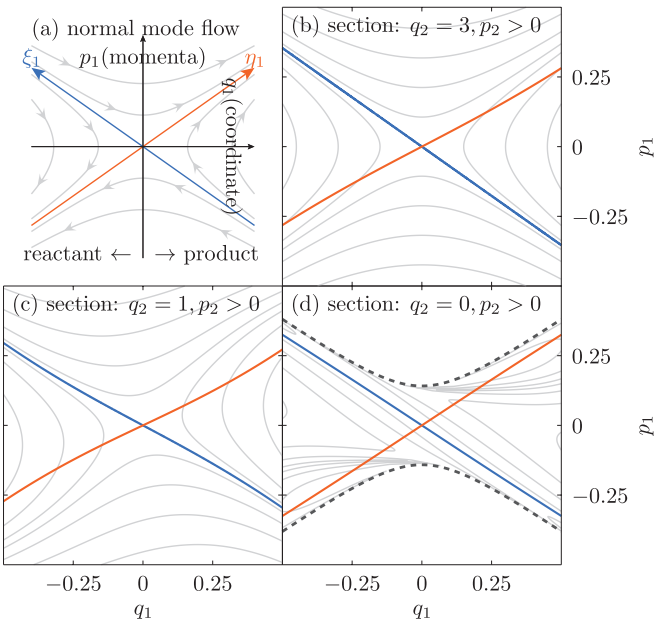

FIG. 1. (Color online) Destination- or origin-dividing set of trajectories sliced on several sections ($q_2 = 0,1,3$ with $p_2 > 0$). Each curve represents a set of trajectories (gray, orange, blue), and each initial condition of the set of trajectories is given by a contour of the value of the action I_1 in the asymptotic region: the initial condition of the destination dividing set of trajectories (blue) is given on that of $q_2 = 5$ with $p_2 > 0$ and propagated backward in time, and that of the origin dividing set of trajectories (orange) is given on the section of $q_2 = -5$ with $p_2 > 0$ and propagated forward in time. Here we have energetically inaccessible region (dashed lines) because of positive kinetic energy $\sum_{j=1}^{n} p_j^2/2$.

run along the hyperbolas given by $I_j = \text{const.}$ shown by gray lines in Fig. 1(a). The η_j and ξ_j axes run along the asymptotic lines of the hyperbolas in Fig. 1(a). One can tell the destination and origin regions of trajectories from the signs of η_j,ξ_j as follows: If $\eta_j > 0$, the trajectory goes into $q_j > 0$ and if $\eta_j < 0$, then the trajectory goes into $q_j < 0$. Therefore one can determine the destination of trajectories from the sign of η_j. Similarly, the origin of trajectories can be determined from the sign of ξ_j. Hereafter we call the set $\eta_j = 0$ "destination-dividing set," $\xi_j = 0$ "origin-dividing set," and each of these sets constitute "reactivity boundaries."

The Hamiltonian of Eq. (1) corresponds to the lowest order (quadratic) part of the Taylor expansion of H. As total energy of the system increases, one needs to consider higher order terms $H_\varepsilon(\boldsymbol{p},\boldsymbol{q})$:

$$H(\boldsymbol{p},\boldsymbol{q}) = H_0(\boldsymbol{p},\boldsymbol{q}) + H_\varepsilon(\boldsymbol{p},\boldsymbol{q}), \tag{3}$$

where H_ε is a power series starting from cubic and higher order terms. Note that, in this case, the actions $\boldsymbol{I}$ are no longer constants of motion. However, previous studies [8–11,16–19] showed that a nonlinear canonical transformation $(p_1,\ldots,p_n,q_1,\ldots,q_n) \to (\bar{p}_1,\ldots,\bar{p}_n,\bar{q}_1,\ldots,\bar{q}_n)$ can provide new action variables as constants of motion, and the associated degrees of freedom are decoupled with each other (to a certain order of approximation) in the new coordinates. Here the new actions and the coordinates are defined in parallel with Eq. (2) by using the newly introduced coordinates $(\bar{\boldsymbol{p}},\bar{\boldsymbol{q}})$:

$$\begin{aligned} \bar{I}_j &= \bar{\xi}_j\bar{\eta}_j, \quad \bar{\eta}_j = (\bar{p}_j + \lambda_j\bar{q}_j)/(\lambda_j\sqrt{2}), \\ \bar{\xi}_j &= (\bar{p}_j - \lambda_j\bar{q}_j)/(\sqrt{2}). \end{aligned} \tag{4}$$

The newly introduced coordinates $(\bar{\boldsymbol{p}},\bar{\boldsymbol{q}})$ are called NF coordinates. The new actions $\bar{I}_j$ are now constants of motion, and consequently the flow around the stationary point follows the contour lines shown in Fig. 1(a), if the axes are changed to the new coordinate $\bar{q}_1$ and $\bar{p}_1$. Thus one can still know the destination and the origin of trajectories from the signs of $\bar{\eta}$ and $\bar{\xi}$. Note that the NF theory is based on the assumption that linear terms dominate dynamics around the saddle and are weakly perturbed by nonlinear terms. Under this assumption λs of the normal modes around a saddle point dominate the dynamics and can extract the integrals of motion if the perturbation calculation converges.

In order to understand whether such reactivity boundaries extracted by NF actually coincide with the true reactivity boundaries that determine the asymptotic behavior of a chemical reaction through index-two saddle, we scrutinize a two DoF model system with an index-two saddle whose higher order term in Eq. (3) is

$$H_\varepsilon(\boldsymbol{p},\boldsymbol{q}) = \varepsilon q_1^2 q_2^2 \exp\left(2 - q_1^2 - q_2^2\right). \tag{5}$$

This nonlinear term is effective locally around $|q_1| = |q_2| = 1$, and vanishes in the asymptotic region($|q_1|$ or $|q_2| = \infty$) and in the vicinity of the saddle ($|q_1|$ and $|q_2| \approx 0$). In what follows, we employ the system parameters as $E = 10^{-2},\varepsilon = 10^{-1},\lambda_1 = 1/\sqrt{2}$, and $\lambda_1 : \lambda_2 = 1 : \gamma$ (golden ratio).

In order to observe the trajectories and the destination- and the origin-dividing sets, we take a set of sections of the phase space at some values of q_j ($j = 1$ or 2). For example, Fig. 1(d) shows the section at $q_2 = 0$ with $p_2 > 0$. There the

gray curves are contour lines of the value of the normal mode action I_j in the asymptotic region. The blue and orange curves are the destination-dividing set and the origin-dividing set, respectively. Numerical extraction of the destination-dividing set is carried out as follows: First, we take a set of points on the line $\eta_1 = 0$ on the section $q_2 = 5$ and $p_2 > 0$. This set divides the destination of the trajectories correctly, and the large positive values of q_2 and the positive sign of p_2 ensure that the trajectories will go into the asymptotic region with positive q_2, where the flows of the trajectories are given by the normal mode Hamiltonian [see Eqs. (3) and (5)], and H_ε becomes negligible for large $|\boldsymbol{q}|$ as shown in Figs. 1(a) and 1(b). The set is then numerically propagated backward in time into the inner region (smaller values of q_2) where the nonlinear term is significant as shown in Figs. 1(c) and 1(d). Similarly, the origin-dividing set is calculated by taking a set of points on $\xi_1 = 0$ on the section of $q_2 = -5$ and $p_2 > 0$ and propagating them forward in time.

Now we compare the numerically calculated destination- and origin-dividing sets with those calculated by the NF theory. Figure 2 shows the destination-dividing set on the section of $q_2 = 0$ with $p_2 > 0$. We observe discrepancy between the numerically calculated set and those of NF ($\bar{\eta}_1^{(3)} = 0$ and $\bar{\eta}_1^{(15)} = 0$, where the upper indices denote the polynomial order of NF). When compared with the normal mode approximation ($\eta_1 = 0$), it is seen that the effect of the nonlinearity is evaluated in the opposite way in the NF compared to the true destination-dividing set. The failure of the NF observed here in calculating the destination-dividing set is not due to the lack of convergence in the perturbation expansion used in the NF theory, because, firstly, the results of the third- and the fifteenth-order of expansion compared in Fig. 2 confirm a good convergence of the NF, and secondly, we have confirmed that the numerically computed trajectories

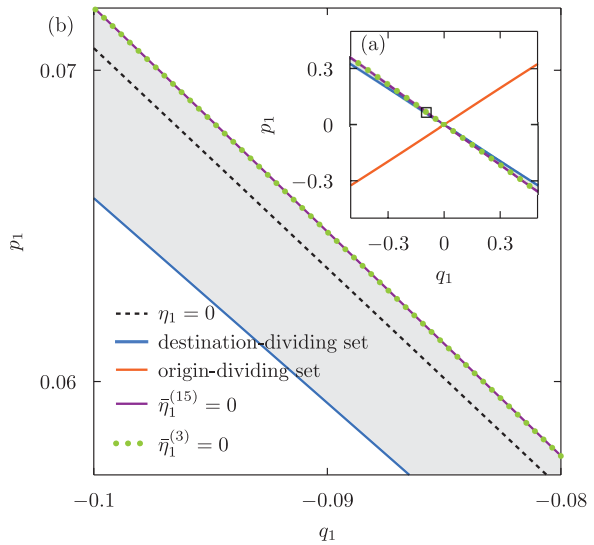

FIG. 2. (Color online) Discrepancy between the numerically extracted destination-dividing set and that of NF $\bar{\eta}_1 = 0$ on the section of $q_2 = 0$ with $p_2 > 0$. Square depicted in (a) denotes the region which are magnified in (b). The shaded areas denote a discrepancy region where the destination is predicted in different ways by the NF and the numerical calculation.

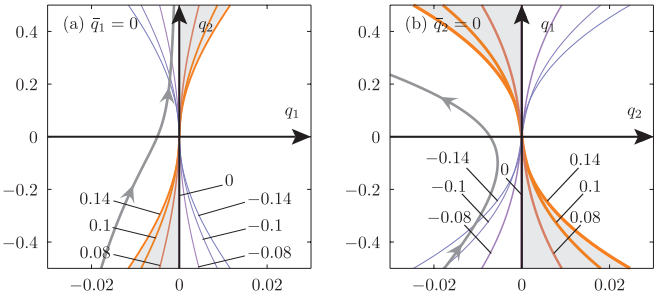

FIG. 3. (Color online) Contour lines of $\bar{q}_1(\mathbf{p},\mathbf{q}|H = E) = 0$ and $\bar{q}_2(\mathbf{p},\mathbf{q}|H = E) = 0$ on the q_1-q_2 space (a) and the q_2-q_1 space (b) with some fixed values of p_1 and p_2 whose values are indicated in the insets. The gray bold curves denote representative trajectories. For instance, the discrepancy regions of $\mathrm{sgn}q_i \neq \mathrm{sgn}\bar{q}_i$ with $p_i = 0.14$ ($i = 1,2$) are denoted by the gray colored areas.

follow the NF destination-dividing set $\bar{\eta}_1 = 0$ in the saddle region, that is, the set $\bar{\eta}_1 = 0$ is truly an invariant set. Thus the NF describes correctly the dynamics of this system, and the sign of $\bar{\eta}_1$ predicts the destination of the trajectory in the $(\bar{q}_1, \bar{p}_1)$ space. However, the "destination" predicted from the sign of the NF coordinate $\bar{\eta}_1$ rather refers to the sign of $\bar{q}_1$ in the future, as can be seen from the discussion in Fig. 1(a). The NF can fail to predict the destination of trajectories when the sign of $\bar{q}_1$ is different from the originally used position coordinate q_1. Figure 3 presents some contour lines of $\bar{q}_1(\mathbf{p},\mathbf{q}|E) = 0$ and $\bar{q}_2(\mathbf{p},\mathbf{q}|E) = 0$ on the q_1-q_2 space and the q_2-q_1 space, respectively, with some fixed values of p_1 and p_2. The right (left) -hand side region of each contour line in the spaces corresponds to a region of $\bar{q}_j > 0$ ($\bar{q}_j < 0$) for fixed p_j [$j = 1$ in Fig. 3(a), $j = 2$ in Fig. 3(b)]. These plots indicate that there exist regions where the signs of $\bar{q}_j$ and q_j are different, and the size of the discrepancy regions ($\mathrm{sgn}q_j \neq \mathrm{sgn}\bar{q}_j$) tends to enlarge with the increase of $|p_j|$ (e.g., see the shaded areas in Fig. 3). Likewise, such failure of the NF also occurs for $\bar{\xi}_1 = 0$ in determining the origin. As Fig. 3 indicates, such a discrepancy can also occur for $\bar{\eta}_2 = 0$ and $\bar{\xi}_2 = 0$. Note, however, that the significance of discrepancy in the NF reactivity boundary is different depending on the instability of these reactive DoFs. Trajectories, denoted by the gray bold curves in Fig. 3, are more strongly repelled along the q_2 direction than q_1 due to the difference of the repulsion ($\lambda_2 > \lambda_1$). The discrepancy between those NF reactivity boundaries and the corresponding destination- and origin-dividing sets is more pronounced along q_1 than along q_2 because trajectories more often enter into the discrepancy region of $\mathrm{sgn}q_1 \neq \mathrm{sgn}\bar{q}_1$ than that of $\mathrm{sgn}q_2 \neq \mathrm{sgn}\bar{q}_2$ due to the difference of the repulsion. Because we interpret this result in terms of the relative magnitudes of the λs without referring to any specific properties of our model, similar results are expected to be found generally in the dynamics around index-two saddles in reacting systems when linear terms dominate dynamics around the saddle and are weakly perturbed by nonlinear terms.

In conclusion, we have numerically constructed the destination- and the origin-dividing sets in a two DoF system with an index-two saddle and compared the results of NF theory with them. We have found the failure of the NF

in identifying the reactivity boundaries especially along the less repulsive DoF even while the perturbation calculation converges. On the other hand, a significant discrepancy was not observed along the strong repulsive DoF, which agrees with Refs. [31,32]. Such a discrepancy could also occur in index-one saddles, although the difference between $\bar{q}$ and q has not been found with significance in index-one saddles [8–13,16–20]. This is probably because, in the case of index-one saddles, there is only one repulsive DoF and all the other DoFs are bound so that trajectories have less possibility to go into the discrepancy regions after leaving the region of the saddle.

In the context of studying dynamics of chemical reaction systems, one needs to divide the asymptotic region of the phase space into "reactants" and "products." For the case of the index-one saddle, this division has seemed trivial because we have only one reactive direction (say, q_1) and therefore only two asymptotic regions ($q_1 \to +\infty$ and $q_1 \to -\infty$). For the case of the higher index saddle, however, we have more than one "reactive" direction, and the division of the phase space is not trivial any more. In this study, to define states we designed a model system that becomes separable in the asymptotic region. In a general case, the asymptotic "reactant" and "product" regions must be assigned by referring to the chemical nature of each specific system such as breaking and formation of chemical bonds. According to the present results, however, such an assignment can be different from those made by NF, especially for less repulsive DoF. Such less repulsive DoF can sometimes serve as the reactive coordinate in molecular systems [28]. This indicates that chemical reactions through higher index saddles can involve much richer structures which require reconsideration of the concepts of "reactant" and "product" themselves. Future works, therefore, will need either to modify the NF reaction theory to remedy the discrepancy between q and $\bar{q}$, or resort to numerical calculations, although the latter is difficult for high DoF systems.

We acknowledge Dr. Yusuke Ootani and Prof. Mikito Toda for their fruitful discussions. This work has been partially supported by the Japan Society for the Promotion of Science. The computations were partially performed using the Research Center for Computational Science, Okazaki, Japan.

[1] S. Glasstone, K. J. Laidler, and H. Eyring, *The Theory of Rate Processes* (McGraw-Hill, New York, 1941).
[2] J. I. Steinfeld, J. S. Francisco, and W. L. Hase, *Chemical Kinetics and Dynamics* (Prentice Hall, New York, 1989).
[3] L. Bonnet and J.-C. Rayez, Int. J. Quantum Chem. **110**, 2355 (2010).
[4] J. Zhang, D. Dai, C. C. Wang, S. A. Harich, X. Wang, X. Yang, M. Gustafsson, and R. T. Skodje, Phys. Rev. Lett. **96**, 093201 (2006).
[5] R. T. Skodje, D. Skouteris, D. E. Manolopoulos, S.-H. Lee, F. Dong, and K. Liu, Phys. Rev. Lett. **85**, 1206 (2000).
[6] W. Shiu, J. J. Lin, and K. Liu, Phys. Rev. Lett. **92**, 103201 (2004).
[7] T. Bartsch, R. Hernandez, and T. Uzer, Phys. Rev. Lett. **95**, 058301 (2005).
[8] T. Komatsuzaki and R. S. Berry, J. Chem. Phys. **110**, 9160 (1999).
[9] T. Komatsuzaki and R. S. Berry, Proc. Natl. Acad. Sci. USA **98**, 7666 (2001).
[10] S. Wiggins, L. Wiesenfeld, C. Jaffé, and T. Uzer, Phys. Rev. Lett. **86**, 5478 (2001).
[11] T. Uzer, C. Jaffé, J. Palacián, P. Yanguas, and S. Wiggins, Nonlinearity **15**, 957 (2002).
[12] C.-B. Li, A. Shoujiguchi, M. Toda, and T. Komatsuzaki, Phys. Rev. Lett. **97**, 028302 (2006).
[13] S. Kawai and T. Komatsuzaki, Phys. Rev. Lett. **105**, 048304 (2010).
[14] R. Hernandez, T. Bartsch, and T. Uzer, Chem. Phys. **370**, 270 (2010).
[15] S. Kawai and T. Komatsuzaki, Phys. Chem. Chem. Phys. **13**, 21217 (2011).
[16] H. Waalkens, R. Schubert, and S. Wiggins, Nonlinearity **21**, R1 (2008).
[17] S. Kawai and T. Komatsuzaki, J. Chem. Phys. **134**, 024317 (2011).
[18] S. Kawai and T. Komatsuzaki, J. Chem. Phys. **134**, 084304 (2011).
[19] Ü. Çiftçi and H. Waalkens, Nonlinearity **25**, 791 (2012).
[20] H. Teramoto, M. Toda, and T. Komatsuzaki, Phys. Rev. Lett. **106**, 054101 (2011).
[21] W.-S. Koon, M. W. Lo, J. E. Marsden, and S. D. Ross, Chaos **10**, 427 (2000).
[22] C. Jaffé, S. D. Ross, M. W. Lo, J. Marsden, D. Farrelly, and T. Uzer, Phys. Rev. Lett. **89**, 011101 (2002).
[23] F. Gabern, W.-S. Koon, J. E. Marsden, and S. D. Ross, Physica D **211**, 391 (2005).
[24] F. Gabern, W.-S. Koon, J. E. Marsden, S. D. Ross, and T. Yanao, Few-Body Syst. **38**, 167 (2006).
[25] M. Toda, T. Komatsuzaki, T. Konishi, R. S. Berry, and S. A. Rice (eds.), *Geometrical Structures of Phase Space in Multidimensional Chaos*, Advances in Chemical Physics, Vol. 130 (John Wiley & Sons, Inc., Hoboken, New Jersey, 2005), and references therein.
[26] T. Komatsuzaki, R. S. Berry, and D. M. Leitner (eds.), *Advancing Theory for Kinetics and Dynamics of Complex, Many-Dimensional Systems*, Advances in Chemical Physics, Vol. 145 (John Wiley & Sons, Inc., Hoboken, New Jersey, 2011).
[27] A. Lichtenberg and M. Lieberman, *Regular and Chaotic Dynamics* (Springer-Verlag, New York, 1992).
[28] R. M. Minyaev, I. V. Getmanskii, and W. Quapp, Russ. J. Phys. Chem. **78**, 1494 (2004).
[29] N. Shida, Adv. Chem. Phys. **130B**, 129 (2005).
[30] D. Heidrich and W. Quapp, Theor. Chim. Acta **70**, 89 (1986).
[31] G. Haller, T. Uzer, J. Palacián, P. Yanguas, and C. Jaffé, Commun. Nonlinear Sci. Numer. Simul. **15**, 48 (2010).
[32] G. Haller, T. Uzer, J. Palacián, P. Yanguas, and C. Jaffé, Nonlinearity **24**, 527 (2011).
[33] G. S. Ezra and S. Wiggins, J. Phys. A: Math. Theor. **42**, 205101 (2009).
[34] P. Collins, G. S. Ezra, and S. Wiggins, J. Chem. Phys. **134**, 244105 (2011).